GEOLOGICA CARPATHICA, DECEMBER 2013, 64, 6, 467–482 doi: 10.2478/geoca-2013-0032

Geochemistry of volcanogenic clayey marine sediments from the Hazar-Maden Basin (Eastern Turkey)

DICLE BAL AKKOCA[1,✉], SEVCAN KÜRÜM[1] and WARREN D. HUFF[2]

[1]Department of Geological Engineering, Faculty of Engineering, Fırat University, Elazığ, Turkey; ✉dbal@firat.edu.tr
[2]Department of Geology, University of Cincinnati, Cincinnati, OH, United States

(Manuscript received January 7, 2013; accepted in revised form October 16, 2013)

Abstract: The Hazar-Maden Basin sediments were deposited along the southern branch of the Neotethys Ocean margin during Late Maastrichtian–Middle Eocene times. X-ray powder diffraction (XRD), ICP-AES, ICP-MS and scanning electron microscopy (SEM) were performed on samples of the Upper Maastrichtian–Middle Eocene Hazar Group and the Middle Eocene Maden Complex from the Hazar-Maden Basin to investigate the main effects of depositional environmental parameters in three sections belonging to deeper marine (slope), proximal arc volcanic (Mastarhill and Yukarıbağ sections) and shallow platform marine (Sebken section) settings. Marine sediments contain clay minerals (smectite, smectite/chlorite, chlorite, illite, interstratified illite/smectite, illite/chlorite, palygorskite), clinoptilolite, quartz, feldspar, calcite, dolomite, opal-CT and hematite. The clays are dominated by iron-rich smectites. La, Zr and Th concentrations are high in the shallow marginal Sebken section where the terrestrial detrital contribution is significant, while Sc and Co are more dominant in the deeper marine (slope) Yukarıbağ section, which is represented by basic-type volcanism and a higher contribution of hydrothermal phases. In a chondrite-normalized REE diagram, the negative Eu anomaly in samples from Sebken, the section which was deposited in a shallow marine environment, is less significant than that of the other two sections indicating the presence of a high terrestrial contribution in that part of the basin. A decrease in $LREE_N/HREE_N$ and La_N/Yb_N, La_N/Sm_N ratios from Sebken to Mastarhill and the Yukarıbağ sections indicates deepening of the basin and an increasing contribution of volcanism in that direction.

Key words: Mastar Mountain, Eastern Turkey, Elazığ area, volcanogenic clayey marine sediments, Neotethys Ocean margin, factor analysis.

Introduction

Marine, volcanic-rich sediments are composed of chemically weathered clay minerals and physically weathered fine-grained rock-forming minerals (Chen et al. 1994). The mineralogical and geochemical signatures of these sedimentary successions have been successfully used to infer constraints on the paleoenvironmental evaluation of some sedimentary basins (Bhatia & Crook 1986). Smectites in volcanic environments are the most important products of the alteration of volcanic detritus (Huff & Turkmenoğlu 1981; Christidis et al. 1995; Huff 2006; Christidis & Huff 2009).

As a result of the northward movement of the Arabian plate towards the Anatolian plate at the beginning of the Late Cretaceous, the southern branch of the Tethys Ocean was subducted to the north, which was recorded in the Hazar Group and Maden Complex (Çelik 2003). Both the Hazar Group and Maden Complex are the key units for understanding the stratigraphic and geodynamic evolution of the region, and therefore, the geologic and stratigraphic characteristics of these units, which are widely exposed around the study area, have been the subject of various works.

The Hazar Basin is filled by marine sediments deposited during Late Maastrichtian–Middle Eocene times. The intensity of volcanic activity increased parallel to the widening of the basin towards the south and east with the Maden Complex being deposited in close association with volcanics. It is different from the Hazar Group. Several models have been suggested for the depositional environment of the basin, which include deep basin deposits (Rigo de Righi & Cortesini 1964), mid-ocean ridge environments (Ileri et al. 1976), plate subduction environments (Yazgan 1984), back arc basins (Hempton 1984), and an island-arc assemblage on a marginal basin (Özçelik 1985). Erdem (1987) studied the petrography of volcanic rocks of the Maden Complex in our study area and Çelik (2003) examined the stratigraphy of units in this basin and proposed a geodynamic evolution of the Hazar-Maden Basin. However, the mineralogy and geochemistry of volcano-sedimentary rocks in the basin have not been studied in detail.

The aim of this study is to use the mineralogical and geochemical characteristics of the Gehroz and Simaki Formations (Hazar Group), Karadere Formation (Maden Complex) in the Hazar-Maden Basin to characterize the distribution of major, trace, and REE elements minerals in the marine sediments. The purpose is to determine the effects of volcanism on the sediments deposited in the Maden Basin and to better describe the geochemistry of the basin with respect to basin depth. Our results might be important for evaluating the depositional environment with regard to stratigraphy as well as geochemical aspects.

This is clearly a topic that is of interest not only to the clay science community, but also to the larger community of geoscientists interested in the Maastrichtian-Eocene history of this region, as well.

Geology

The study area is located on the Mastar Mountain to the southeast of Elazığ (Eastern Turkey) (Fig. 1a). The units exposed in the study area, include the Upper Jurassic-Lower Cretaceous Guleman Ophiolites, Senonian Elazığ magmatic rocks, Upper Maastrichtian-Middle Eocene Hazar Group, the Middle Eocene Maden Complex, Pliocene-Quaternary, and recent alluvial fans and river bed alluvium deposits (Fig. 1b).

The Guleman Ophiolites are composed of, dunite, harzburgite with podiform chromite, alternating dunite-wherlite-clinopyroxenite banded gabbro, quartz gabbro/diorite or

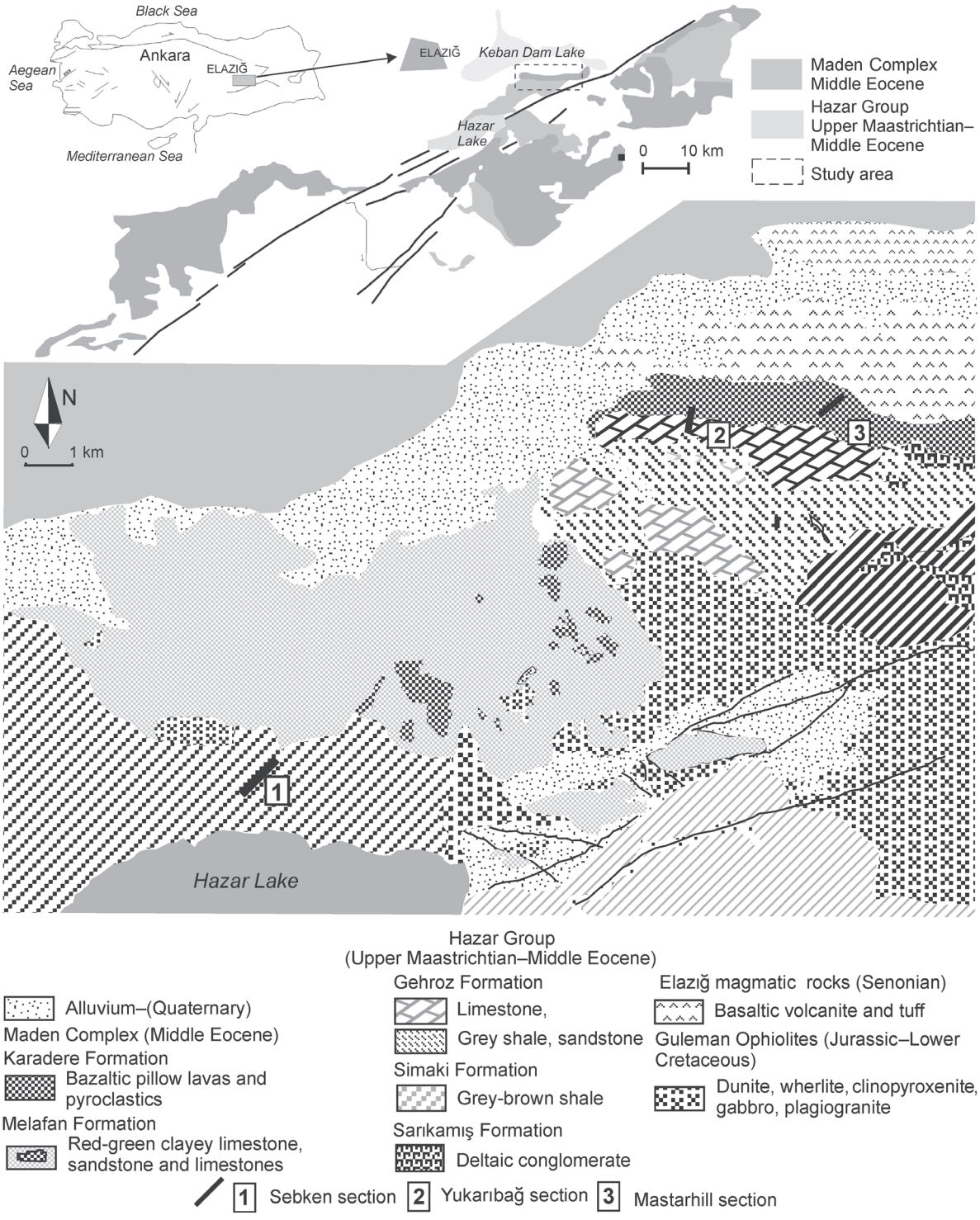

Fig. 1. a — Simplified geological map of the Hazar Group and Maden Complex from Eastern Anatolia; **b** — Geological map of the study area, showing the location of the sampled sections in the Hazar-Maden Basin (simplified from Erdem 1987 and Çelik 2003).

plagiogranite and volcanites. These do not show any field relation with ophiolites but are thought to be genetically related to oceanic crust (Erdoğan 1977; Özkan & Öztunalı 1984).

The Elazığ magmatic rocks exposed largely in the Elazığ region contain plutonic rocks composed of diorites, monzodiorites, quartz-diorites, and tonalites, volcanic rocks (composed of basaltic pillow-lavas), andesitic lavas, and andesitic pyroclastic rocks. The geochemical studies indicate that the Elazığ magmatic rocks generally belong to a calc-alkaline series and that they are the products of island-arc magmatism (Yazgan 1984; Yazgan & Chessex 1991).

The lowest part of the Hazar Group consists of the Sarıkamış Formation containing conglomerate that laterally and vertically transitions to limestone, and the Simaki Formation consisting of sandy limestone and grey-brown shales. Çelik (2003) suggests that this formation was deposited in shallow parts of the Hazar-Maden Basin. The Simaki Formation is overlain by the Gehroz Formation which consists of limestone and interbedded shale and sandstone. The Simaki Formation in the Sebken section represents shallower parts of the marine basin and it is transitional to the Gehroz Formation with a deep facies character in the lower levels of the Mastarhill section to the east (Erdem 1987).

The Maden Complex conformably lying on the Hazar Group was formed in an E-W trending extensional basin during the Middle Eocene. During the rifting stage of the basin, calc-alkaline volcanism accompanied the marine clastic deposits and the lithology changed to reef limestones. Rapid subsidence of the basin led to deposition of overlying pelagic deposits that include thin layered red limestone, shale and mudstone (Erdoğan 1977; Özçelik 1982; Aktaş & Robertson 1990; Yılmaz 1993). The Maden Complex has a complex lithology consisting of limestones, red-green clayey limestones, sandstone of the Melefan Formation and agglomerate, tuffs, reddish mudstone and basaltic-andesitic pillow lavas of the Karadere Formation. The upper levels of the Mastarhill section and the Yukarıbağ section correspond to the Karadere Formation. Erdem (1987) notes that the volcanites are composed of basalts and andesites. Mn is depleted in the Mastarhill volcano-sedimentary units, while the volcano-sedimentary rocks in the Yukarıbağ section contain evidence of Mn mineralization. Altunbey & Sağıroğlu (1995) identified several opaque minerals such as pyrolusite, psilomelane, braunite, manganite plus manganiferous minerals, hematite, magnetite and chromite in the assemblage. Hematite, magnetite, chromite, and pyrite also occur surrounding mudstones.

Fluvial deposits of Pliocene age form the youngest unit in the study area. This unit is unconformably overlain by Pliocene–Quaternary and recent alluvial deposits (Çelik 2003).

Material and method

Thirty samples were collected from the Yukarıbağ, Mastarhill and Sebken measured stratigraphic sections where clayey rocks of the Hazar Group and clayey and volcaniclastic rocks of the Maden Complex are widely exposed. The Sebken section consists of the Simaki Formation, the Mastarhill section consists of the Gehroz and the Karadere Formations, and the Yukarıbağ section consists of the Karadere Formation.

The bulk mineralogy was determined by X-ray powder diffraction (XRD) (Rigaku DMAXIII), using Ni-filtered Cu Kα at 15 kV–40 mA instrumental settings.

The clay particles (<2 μm) were separated by centrifuge after dispersion by sedimentation. Carbonate was removed from pulverized rocks using hydrochloric acid treatment. Clay mineralogy was determined by XRD by using oriented samples after air-drying, saturation with ethylene glycol for 12 h and heating at 490 °C for 4 h. The assignment of diffraction maxima was based on the standard International Centre for Diffraction Data (JCPDS) file.

The whole-rock mineral percentages were determined following the technique described by Gündoğdu (1982) after Brindley (1980). In this method, all samples were mounted in random and oriented mounts. The characteristic peak intensities (I) of minerals were normalized to that of the (104) reflection of dolomite. In other words, a K factor for each mineral (including clays with peaks between 19 and 20° Θ) was determined as $K = I_{dolomite}/I_{mineral}$ in a 1 : 1 dolomite mineral mixture by weight. Percentages of the minerals were calculated from the following equation: % of mineral $a = 100 \times K_a \times I_a / (K_a \times I_a + K_b \times I_b) + \ldots . K_n \times I_n)$. The relative error of this method is less than 15 %.

The relative abundances of whole-rock minerals were estimated by weighting integrated peak areas of characteristic *basal reflections* in the air-dried with the empirical factors of Gündoğdu (1982) after Brindley (1980). The characteristic peak intensities (I) of the minerals were normalized to that of the (104) reflection of dolomite. Accordingly, the areas of the air dried 3.04 Å peak were multiplied by 0.74 to yield calcite, the area of the 3.34 Å peak was multiplied by 0.34 to obtain quartz, the 3.20 Å peak areas were multiplied by 1.62 to estimate feldspar, the 4.48 Å peak areas were multiplied by 14.63 to yield clay minerals, the 4.04 Å peak areas were multiplied by 2.72 to yield opal-CT. The accuracy of this method is within 15 %.

Clay minerals were *estimated* by *weighting integrated peak areas* of characteristic *basal reflections* in the glycolated state with the *empirical factors* of Gündoğdu (1982) after Brindley (1980). The characteristic peak intensities (I) of the minerals were normalized to that of the (104) reflection of dolomite. Accordingly, the areas of the glycolated 5.7 Å peak were multiplied by 0.81 to yield smectite, the area of the 5.0 Å peak was multiplied by 0.51 to obtain illite, the 6.4 Å peak areas were multiplied by 1.00 to estimate palygorskite, the 7.8 Å peak areas were multiplied by 0.83 to yield smectite/chlorite (S-C), the 5.4 Å peak areas were multiplied by 0.66 to yield illite/smectite (I-S). The relative accuracy of this method is within 15 %.

Chemical data were obtained for 30 representative samples at Acme Analytical Laboratories Ltd. (Canada) using ICP-AES for the determination of major and trace elements and ICP-MS for rare-earth elements (REE). Samples were crushed to approximately 0.5 cm and then approximately half the sample was pulverized to minus 100 mesh. A 30-gram sample was digested with 3 ml of 3–1–2 $HCl–HNO_3–H_2O$ at 95 °C for one hour and diluted with water. Major elements

are expressed as oxide percents (i.e. SiO_2, Al_2O_3, CaO, Cr_2O_3, total Fe_2O_3, K_2O, MgO, MnO, Na_2O, P_2O_5 and TiO_2). Other element concentrations are given in ppm. Loss on ignition was determined by weight difference after ignition at 1000 °C. In whole-rock analysis, feldspar was identified using reflections at 3.16 Å, dolomite at 2.92 Å, calcite at 3.03 Å, quartz at 3.33 Å, hematite at 2.69 Å, and opal-CT at 4.04 Å peaks (Fig. 2a). Mineral compositions were determined on the <2 μm fractions obtained by the sedimentation of M21 samples, with smectite content (80 %), respectively, followed by centrifugation of the suspension up at 15,000 rpm for 15 minutes, after soaking in distilled water overnight. Major oxides were determined with a Varian Vista MPX ICP-OES. Structural formulas were computed on the basis of 11 oxygen atoms for smectite (Weaver & Pollard 1973).

Representative clay-rich freshly broken samples were used for SEM–EDX analysis with a LO-435 VP SEM. The samples (gold coated) were attached to aluminium holders using double-sided tape.

Statistical analyses were carried out using the statistical package for the social sciences (SPSS) 8.0 statistical program. Correlation coefficients were calculated from the data set of the geochemical analyses. Accordingly, the significance level is $\alpha = 0.05$ with correlation coefficients (r) of 0.30. Factor analyses were applied to major and trace elements to get a small set of variables (preferably uncorrelated) from a large set of variables (most of which are correlated with each other). Analysis was performed by principal components afterwards and the rotation of the principal components was carried out by the varimax normalized method (Kaizer 1960).

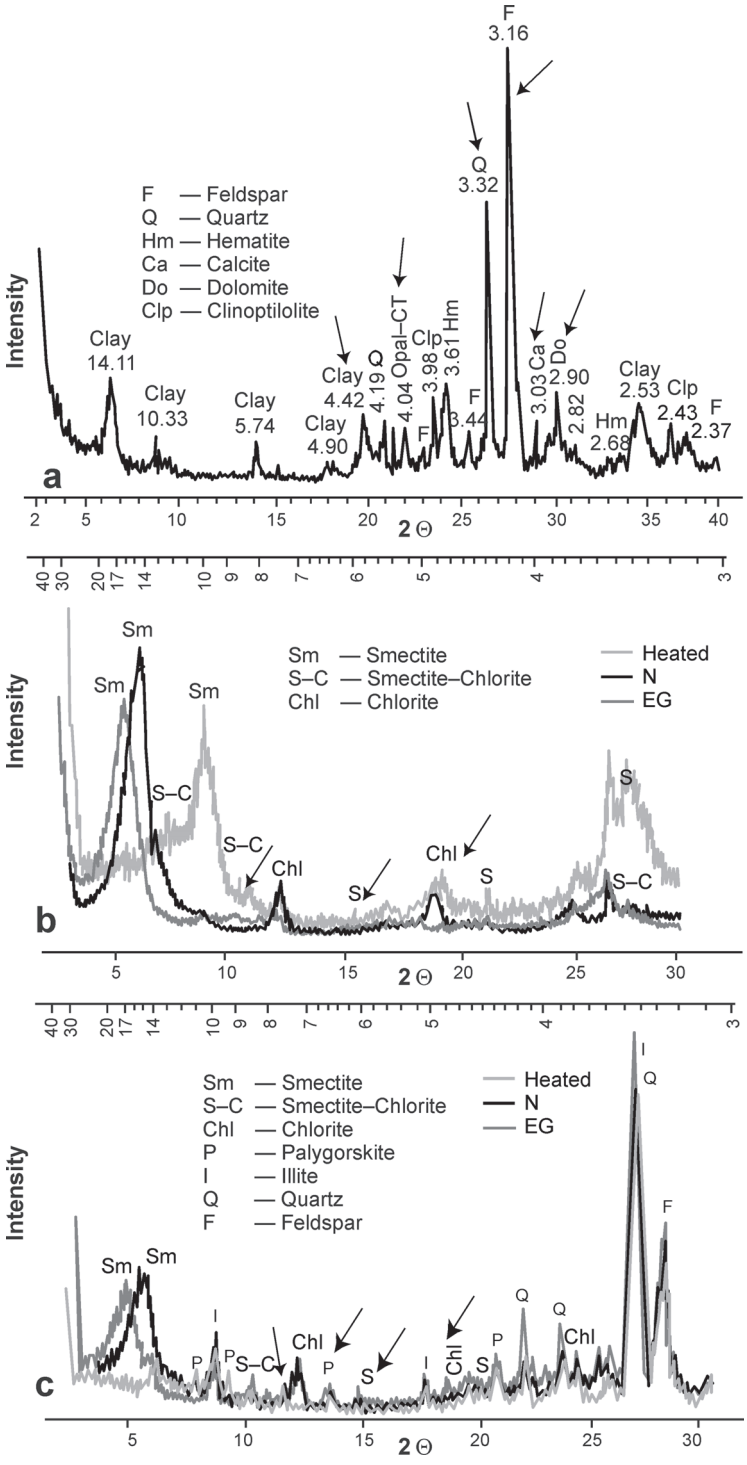

Fig. 2. XRD patterns of representative samples: **a** — M24, **b** — M1, **c** — Y1. The characteristic peak intensities (I, arrow) of minerals were normalized to that of the (104) reflection of dolomite for semiquantitative analyses of whole-rock minerals according to Gündoğdu (1982) after Brindley (1980).

Results

X-ray diffraction

The results from X-ray diffraction analysis on both whole-rock and clay fractions of 29 samples from the Sebken, Mastarhill and Yukarıbağ sections are listed in Table 1. All samples consist of clay minerals (smectite, smectite/chlorite (S-C), chlorite, illite, interstratified illite/smectite (I-S), illite/chlorite (I-C), palygorskite), quartz, feldspar, calcite, dolomite, opal-CT and hematite. Clayey rocks are dominated by smectite, chlorite and S-C in Sebken and Mastarhill. Chlorite is most abundant in the Yukarıbağ section. I-C is present only in S4 and S6 samples from Sebken, I-S is in S16 sample from Sebken and M17 sample from the Mastarhill sections.

The d-spacing of air dried smectite peaks is in the range of 15.0–15.9 Å, which swelled to 17.5–18.0 Å when glycolated. Heating (490 °C) caused a collapse to 10 Å (Fig. 2b,c). Spacing values at 15.0–15.9 Å for the (001) indicate that smectite is of the Ca-type (Moore & Reynolds 1989) (Fig. 2b,c). The position of 060 peaks showed the dioctahedral character (d060 = 1.49–1.51 Å).

Table 1: Whole-rock and clay fraction mineral percentages of samples from Sebken (**a**), Mastarhill (**b**) and Yukarıbağ sections (**c**). **Feld.** — Feldspar, **Dolo.** — Dolomite, **Hema.** — Hematite, **Op.-CT** — Opal-CT, **Smec.** — Smectite, **Chl.** — Chlorite, **S-C** — Smectite-Chlorite, **I-S** — Illite-Smectite, **I-C** — Illite-Chlorite, **Paly.** — Palygorskite, **n** — Sample number, **General Mean** — Total/n.

a	**Whole-rock minerals**					**Clay minerals**							
Sebken (n=11)	**Quartz**	**Feld.**	**Calcite**	**Dolo.**	**Clay**	**Op.-CT**	**Smec.**	**Illite**	**Chl.**	**S-C**	**I-S**	**I-C**	**Paly.**
S1	7	20	–	4	65	4	–	22	–	35	–	–	43
S4	11	7	19	–	60	3	14	19	–	43	24	–	–
S9	15	5	33		47	–	–	29	48	23	–	–	–
S12	14	10	25	3	41	7	–	17	56	27	–	–	–
S14	18	6	25	–	51	–	17	12	36	35	–	–	–
S16	12	9	–	2	68	9	–	11	25	19	14	8	23
S20	13	11	29	–	40	7	24	–	–	76	–	–	–
S28	9	5	71	–	6	9	78	–	–	–	–	–	–
S38	9	6	76	–	9	–	83	–	–	–	–	–	17
S41	10	5	34	–	49	–	13	17	42	28	–	–	–
S44	9	10	13	–	63	5	14	16	–	40	–	–	30
General Mean	11.54	8.54	29.54	0.81	43.36	4	26.88	15.88	23.0	36.22	1.55	3.55	10.77

b	**Whole-rock minerals**						**Clay minerals**					
Mastar (n=11)	**Quartz**	**Feld.**	**Calcite**	**Dolo.**	**Clay**	**Op.-CT**	**Smec.**	**Illite**	**Chl.**	**S-C**	**I-S**	**Paly.**
M1	8	13	57	–	22	–	6	–	85	9	–	–
M4	7	18	16	–	59	–	89	–	–	11	–	–
M6	15	12	37	–	26	10	–	–	51	49	–	–
M7	12	16	24	–	43	5	66	21	13	–	–	–
M9	4	17	79	–			16	11	34	39	–	–
M13	7	13	26	–	39	2	81	–	–	19	–	–
M17	11	7	18	–	61	3	–	17	30	24	12	17
M19	12	15	10	5	52	6	17	10	34	39	–	–
M21	5	25	9	3	58		33	19	–	48	–	–
M24	5	27	2	3	61	2	46	24	–	30	–	–
M25	9	11	15	2	55	8	11	13	22	28	–	–
General Mean	8.63	15.81	26.63	1.18	43.27	3.27	52.14	13.0	42.14	42.0	1.71	6.14

c	**Whole-rock minerals**							**Clay minerals**				
Yukarıbağ (n=7)	**Quartz**	**Feld.**	**Calcite**	**Dolo.**	**Clay**	**Op.-CT**	**Hema.**	**Smec.**	**Illite**	**Chl.**	**S-C**	**Paly.**
Y1	8	9	3	2	78	–	–	16	34	33	–	19
Y2	4	2	–	17	30	–	47	16	–	84	–	–
Y3	23	10	–	–	67	–	–	–	15	51	34	–
Y4	2	22	5	8	51	12	–	21	13	44	22	–
Y11	5	12	–	–	83	–	–	–	20	80	–	–
Y12	8	26	–	–	66	–	–	24	17	39	20	–
Y14	9	13	–	6	72	–	–	11	5	76	8	–
General Mean	8.57	13.85	1.14	3.14	71.57	1.71		7.57	15.14	58.14	8.0	2.71

The 12–12.5 Å (002) peaks in air dried XRD patterns of illite/smectite expand to 13.5 Å in glycolated samples and collapse to 10 Å in heated samples (Fig. 2b). Peaks at 10 Å, 5 Å and 3.35 Å in the normal XRD pattern of illite did not change upon glycolation and heating.

Chlorite shows characteristic peaks at 14 Å, 7.06 Å, 4.77 Å which remain unchanged in air dried and glycolated XRD patterns. The intensity of the 7 Å peak decreases in heated samples. The relatively low intensity of odd order reflections reveals that chlorite is Fe-rich (Brindley 1980). The peak at 7 Å in air dried patterns of smectite/chlorite mixed layers are wider and broader than those of chlorite and they are easily distinguished with glycolated and heated patterns. Heated (12 Å) peaks of (002) separate smectite-chlorite from the chlorite. Peaks of illite/chlorite do not change in normal and glycolated patterns but in heated samples the (002) peak is lowered from 14.2 Å to about 12–12.5 Å.

Palygorskite is a common mineral in samples, and a 10–10.4 Å peak in the air dried pattern did not change in the glycolated pattern but collapsed to 9 Å after the heat treatment (Fig. 2c).

SEM results

The most abundant carbonate mineral is calcite, which is present in the form of spherical or rounded crystals up to 1–6 μm in length (Fig. 3a.).

Smectites appear to grow on vesicular volcanic glass shards in the form of flakes on *popcorn*-shaped spongy hyaloclasts or spherical authigenic forms (Fig. 3b). Spherical alteration and volcanic glass shards are very common, where smectite developed from glassy tuffs (Fig. 3c–d).

Chemical composition of clay minerals

The chemical composition of smectite in sample M4 is given in Table 2. It is characteristic of this smectite that the main octahedral cation is Mg and Fe. The Mg/(Fe+Mg) ratio is 0.4–0.75

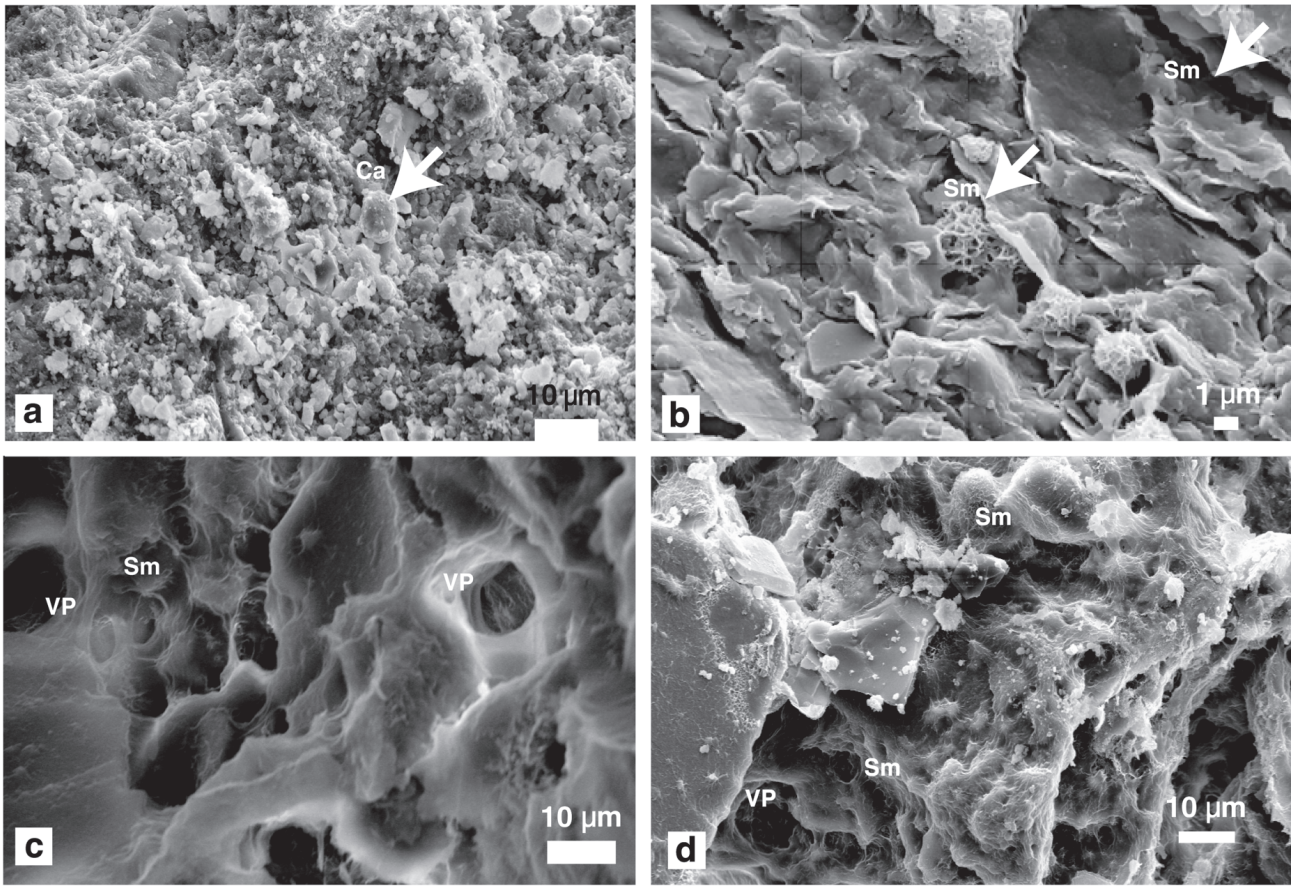

Fig. 3. SEM pictures of **a**) mosaic of euhedral (rhombic) and subeuhedral calcite crystals (Ca), with a spherical or rounded habit and variable size and shape **b–c–d**) spherical authigenic smectites (Sm). Smectites replace volcanic glass and rim intergranular pores (VP).

Table 2: Major element compositions and structural formula of smectite from the M4 sample. Structural formulas were computed on the basis of 11 oxygen atoms for smectite. **ΣFe_2O_3** — total iron, **LOI** — loss on ignition, **TC** — tetraeder charge, **OC** — octaeder charge, **TOC** — total octaeder cation, **ILC** — interlayer charge, **TLC** — total layer charge.

SiO_2	TiO_2	Al_2O_3	ΣFe_2O_3	MnO	Cr_2O_3	NiO	MgO	CaO	Na_2O	K_2O	P_2O_5	LOI	Total
41.08	1.74	8.61	18.62	0.22	0.02	0.12	9.61	2.34	0.85	0.91	0.12	15.93	100.17

Tetraeder		Octaeder							Interlayer					TC	TOC	OC	ILC	TLC
Si	Al	Ti	Al	Fe	Mn	Cr	Ni	Mg	Mg	Ca	Na	K	P					
3.23	0.77	0.10	0.03	1.10	0.02	–	0.01	1.13	0.06	0.20	0.13	0.09	0.01	0.77	2.33	0.01	0.79	0.78

in octahedral cations, and it can be attributed to trioctahedral smectite which corresponds to Fe-saponite composition.

The composition of smectite depends on the nature of the parent mineral and the surrounding material (Wiewiora 1978). The Mg, Fe, Ni and Cr concentrations of the samples provide some evidence for the parent material of smectites. High amounts of these elements in samples are present in octahedral sites and these results are interpreted as representing smectite formation from basaltic rocks as the Fe-rich gels react with solid particles and dissolved species (Köster et al. 1999). High concentrations of Mn, Ti and Fe are attributed to Mn-Fe-Ti oxides in the clay phase. The K_2O concentration in the clay fraction is 0.91, and it does not correspond to a typical smectite composition (Weaver & Pollard 1973). The amount of K concentration in smectite depends upon the illite content in the mixed-layer phase. Smectite illitization is a common mineralogical reaction occurring during the burial diagenesis of clay-rich sediments and shales (Lanson et al. 2009).

Whole-rock geochemistry

Major and trace elements

Major and trace element concentrations of the studied samples are listed in Table 3.

Table 3: Major and trace element contents and La/Sc, Th/U, Sc/Th, Co/Th, Zr/Hf ratios in samples of the Sebken, Mastarhill and Yukarıbağ sections. ** — average of all samples. Fe_2O_3 is total Fe as Fe_2O_3. *Continued on the page 474.*

Sample No.		Concentration (wt. %)												
		SiO_2	Al_2O_3	Fe_2O_3	MgO	CaO	Na_2O	K_2O	TiO_2	P_2O_5	MnO	Cr_2O_3	LOI	Total
Sebken	S-1	51.48	16.98	9.66	3.81	2.19	2.41	2.25	0.91	0.14	0.22	0.038	9.7	99.79
	S-4	48.55	14.56	9.57	4.53	5.74	0.52	1.86	0.8	0.14	0.18	0.049	13.2	99.78
	S-9	41.98	10.02	6.56	4.56	16.5	0.42	1.3	0.74	0.1	0.20	0.066	17.3	99.78
	S-12	40.7	10.08	6.42	3.28	17.7	1.09	1.08	0.63	0.11	0.12	0.027	18.6	99.81
	S-14	50.8	12.45	8.69	4.02	7.38	0.62	1.39	0.86	0.15	0.2	0.031	13.2	99.81
	S-16	49.01	14.91	11.56	5.01	1.55	0.66	1.85	0.93	0.17	0.27	0.083	13.7	99.75
	S-20	39.98	10.63	8.35	5.67	14.11	0.97	1.18	0.88	0.16	0.11	0.066	17.6	99.76
	S-28	27.91	7.17	4.36	2.39	29.49	1.47	0.82	0.39	0.11	0.2	0.016	25.5	99.82
	S-38	15.49	2.45	1.64	1.34	43.05	0.15	0.39	0.13	0.09	0.15	0.009	34.9	99.77
	S-41	43.61	11.96	7.36	3.96	12.95	0.59	1.55	0.73	0.13	0.18	0.043	16.7	99.8
	S-44	49.18	14.06	8.52	4.67	6.88	1.15	1.99	0.84	0.15	0.16	0.037	12.1	99.78
	Average	41.69	11.38	7.51	3.93	14.32	0.91	1.42	0.62	0.13	0.18	0.04	17.5	99.78
Mastarhill	M-1	20.06	4.92	2.35	3.2	35.92	1.21	0.47	0.22	0.05	0.06	0.015	31.4	99.88
	M-4	39.4	9.3	8.03	8.41	13.63	1.08	0.79	0.65	0.1	0.11	0.187	18	99.72
	M-6	38	9.2	7.42	6.92	16.57	0.86	1.15	0.69	0.12	0.12	0.046	18.6	99.74
	M-7	44.43	10.89	7.9	5.84	11.76	1.19	1.28	0.82	0.12	0.15	0.089	15.3	99.76
	M-9	21.73	4.2	2.79	2.24	36.04	0.95	0.7	0.3	0.09	0.12	0.04	30.6	99.8
	M-13	45.45	14.13	9.91	6.43	5.53	0.97	2.19	1.01	0.17	0.08	0.071	13.8	99.74
	M-17	46.05	13.64	9.16	4.54	9.06	1.71	1.44	0.77	0.08	0.14	0.029	13.2	99.79
	M-19	49.81	13.26	9.48	5.38	7.24	1.57	1.4	1.04	0.13	0.17	0.058	10.2	99.77
	M-21	50.08	16.45	8.08	4.49	6.49	2.51	1.71	0.50	0.06	0.13	0.004	9.3	99.77
	M-24	54.42	16.86	8.11	4.62	3.24	3.1	2.09	0.57	0.07	0.13	0.004	6.5	99.75
	M-25	56.69	14.49	8.89	4.29	2.24	1.77	2.76	0.79	0.1	0.13	0.036	7.6	99.8
	Average	42.37	11.57	7.46	5.12	13.42	1.53	1.45	0.66	0.09	0.12	0.052	15.86	99.77
Yukarıbağ	Y-1	39.45	14.12	9.49	4.69	14.59	3.43	0.71	1.21	0.11	0.24	0.032	11.7	99.79
	Y-2	18.63	5.36	43.35	1.71	7.52	0.09	0.19	0.2	0.92	16.21	0.009	5.1	99.35
	Y-3	59.71	14.2	8.08	5.22	0.82	0.99	2.04	0.77	0.12	0.3	0.031	7.5	99.78
	Y-4	44.8	13.95	8.33	10.2	9.17	1.41	0.29	0.63	0.17	0.24	0.109	10.4	99.72
	Y-11	50.48	17.94	10.09	3.33	1.68	0.96	5.04	1	0.12	0.1	0.011	9.1	99.83
	Y-12	45.26	17.65	8.93	6.66	3.27	0.44	3.53	0.92	0.07	0.2	0.014	12.8	99.77
	Y-14	35.64	14.27	7.29	7.46	13.99	0.16	3.21	0.85	0.1	0.2	0.041	16.5	99.76
	Y-16	1.37	0.36	0.18	0.8	54.12	0.02	0.07	0.02	0.04	0.01	0.003	42.9	99.92
	Average	36.91	12.23	11.96	5.0	13.14	0.93	1.88	0.70	0.20	2.18	0.031	14.5	99.74

Sample No.		Concentration (ppm)										
		Ni	Sc	Ba	Co	Cs	Ga	Hf	Nb	Rb	Sr	Ta
Sebken	S-1	148	32	146	38.9	2.3	15.5	2.6	7.8	50.9	191.9	0.5
	S-4	247	26	291	45.9	4	15.1	2.9	14.8	61	80.4	0.8
	S-9	259	17	254	23.9	2.2	12.4	3.2	13.5	40	195.7	0.9
	S-12	109	18	296	23.4	1.7	12.4	2.2	11.8	29.2	242.8	0.7
	S-14	174	20	172	37.5	2.2	15.1	2.9	20.2	44.6	87	1.2
	S-16	429	33	266	58	3.3	17	3.9	15.9	57.8	72.1	1.1
	S-20	375	21	123	50	1.7	11.9	3.2	16.3	37.5	306	0.9
	S-28	74	12	353	17.3	1.2	7.6	1.7	5.9	23.7	337.1	0.4
	S-38	60	4	991	10.4	0.3	5.5	0.5	2.7	12.2	506.3	0.1
	S-41	186	21	236	35.8	2.6	14	2.5	11.8	47.4	106.8	0.7
	S-44	171	26	195	41.6	3.6	15.9	3.1	14.4	57.3	143.7	0.8
	Average	202.90	20.90	302.09	34.79	2.28	12.94	2.60	12.28	41.96	206.34	0.73
Mastarhill	M-1	43	12	27	9.2	0.5	7.7	0.8	0.6	7.8	401.2	0.1
	M-4	614	21	73	58.3	1	10.6	1.5	9.9	18.4	520.1	0.5
	M-6	265	20	106	27.6	1.1	11.3	2.1	11.4	29	488.2	0.7
	M-7	327	22	135	46.1	1.7	11.9	2.6	13.9	36.7	343.5	0.9
	M-9	74	8	59	11.9	0.5	6.4	1.1	3.5	15.6	1115.1	0.2
	M-13	337	30	191	49.9	4.2	15.4	3.1	17.2	74.3	141.7	1
	M-17	97	29	114	34.9	1.8	13.9	1.9	7.6	41.8	226.3	0.5
	M-19	201	25	80	36	1.5	15.1	3.3	24.9	41.9	256.8	1.6
	M-21	20	30	163	26.7	0.6	14.4	3.9	25	30.4	213.8	1.6
	M-24	20	30	154	25.3	1.2	15.5	3	17.7	35.1	422.5	0.9
	M-25	123	27	153	26.8	3.2	16	3.5	21.4	69	189	1.4
	Average	192.8	23.0	114.0	32.06	1.57	12.5	2.43	13.91	36.36	392.56	0.85
Yukarıbağ	Y-1	102	31	58	37.5	0.2	12	2.2	2.3	9.3	277.7	0.1
	Y-2	795	10	92	63.8	0.1	30.2	1.7	5.7	2.6	387.7	0.1
	Y-3	202	21	203	41.8	3.9	20.4	2.9	12.1	78.2	47.4	0.7
	Y-4	280	34	233	46.7	0.1	13.2	1.4	9.6	5	261.1	0.3
	Y-11	79	41	281	39.4	2.8	15.2	1.6	9.4	72.7	81.9	0.4
	Y-12	73	39	240	39.9	2.3	16.5	2	9.3	57.5	130	0.5
	Y-14	98	35	130	35.5	0.4	14.1	1.4	7.4	47.9	80.4	0.2
	Y-16	20	1	8	0.9	0.1	1.3	0.2	0.3	1.4	550.6	0.1
	Average	206.12	26.5	155.62	38.18	1.23	15.36	1.67	7.01	34.32	227.1	0.3

Table 3: *Continued.*

	Sample No.	Th	U	V	Zr	Y	Cu	Pb	Zn	As
Sebken	S-1	4.5	0.9	198	98.1	25.9	81.6	16.4	91	5.7
	S-4	5.3	1.2	174	110.3	19.9	63	20	106	5.5
	S-9	4.9	1.4	120	112.3	18.9	38.1	3.1	79	0.5
	S-12	3.2	0.9	132	76.3	16.8	35.6	10	76	10.3
	S-14	5.5	0.9	151	109.2	20.4	58.3	7.1	83	0.8
	S-16	5.1	1.7	214	143.5	28.5	61.8	14.7	93	8.2
	S-20	3.1	1.3	153	99.7	18.7	43	6.5	72	18.2
	S-28	3.9	0.7	70	60.8	17.6	10.7	9.4	52	2.8
	S-38	1.8	0.3	23	21.9	13.1	24.8	9.5	29	0.9
	S-41	4.0	1.1	148	87.3	19.8	68	13.5	81	5.8
	S-44	4.3	0.9	178	101.4	20.6	70.6	10	83	6.5
	Average	4.15	1.03	141.91	92.80	20.02	50.50	10.93	76.82	5.93
Mastarhill	M-1	0.2	1.3	87	14.4	6.6	8.7	1.4	15	1.2
	M-4	2.0	0.8	148	61.3	14.1	44.5	5.9	72	6.3
	M-6	3.0	1.0	139	76.1	18.5	46.6	2.7	71	3.2
	M-7	3.2	1.0	163	95.7	20	48.8	6.9	84	5
	M-9	1.2	0.9	60	31.6	8.9	16.1	2.5	27	4.4
	M-13	4.7	1.5	212	111.1	22.8	73.2	7.1	100	6.3
	M-17	2.8	0.5	200	66.9	17.4	64.8	7.3	87	0.6
	M-19	4.7	1.4	197	119.7	19.6	60.1	2.7	87	2.7
	M-21	3.3	1.1	204	138.8	26	49.5	3.6	69	1.9
	M-24	2.4	0.9	254	109.7	23.1	116.6	3.9	72	4.9
	M-25	3.9	0.9	169	119.5	22.4	20.5	8	74	15.5
	Average	2.85	1.03	166.64	85.89	18.13	49.95	4.73	68.91	4.73
Yukarıbağ	Y-1	0.2	0.1	245	80	23.4	40.8	2.2	56	3.1
	Y-2	2.6	3.4	1465	112	144.1	872.3	219	492	249
	Y-3	7.0	1.4	162	103.1	19.2	144	5.8	111	1.5
	Y-4	1.6	0.4	198	42.7	13	92.8	1.6	48	1.8
	Y-11	1.8	0.6	79	65.3	15.5	14.4	1.6	37	2
	Y-12	1.7	0.5	211	61.9	14.8	112.1	1.9	55	0.8
	Y-14	1.5	0.6	178	53.8	15.4	152	1.1	50	0.5
	Y-16	0.2	0.8	8	2.5	2.7	3.2	0.5	4	0.9
	Average	2.1	1.0	318.3	65.2	31.0	179.0	29.2	106.6	32.5

	Sample No.	Th/U	Zr/Hf	Y/Ho
Sebken	S-1	5.00	37.73	27.55
	S-4	4.42	38.03	26.18
	S-9	3.50	35.09	28.64
	S-12	3.56	34.68	30.00
	S-14	6.11	37.66	29.57
	S-16	3.00	36.79	29.38
	S-20	2.38	31.16	30.16
	S-28	5.57	4.00	32.00
	S-38	6.00	43.80	34.47
	S-41	3.64	34.92	29.12
	S-44	4.78	32.71	27.84
	Average	4.36	33.33	29.54
Mastarhill	M-1	0.15	18.00	27.50
	M-4	2.50	40.87	29.38
	M-6	3.00	36.24	29.84
	M-7	3.20	36.81	28.17
	M-9	1.33	28.73	31.79
	M-13	3.13	35.84	28.15
	M-17	5.60	35.21	27.19
	M-19	3.36	36.27	26.13
	M-21	3.00	35.59	27.66
	M-24	2.67	36.57	27.50
	M-25	4.33	34.14	28.00
	Average	2.93	34.02	28.30
Yukarıbağ	Y-1	2.00	36.36	27.21
	Y-2	0.76	65.88	23.78
	Y-3	5.00	35.55	26.67
	Y-4	4.00	30.50	26.53
	Y-11	3.00	40.81	25.41
	Y-12	3.40	30.95	24.87
	Y-14	2.50	38.43	26.55
	Y-16	0.25	12.50	37.57
	Average	2.61	36.37	26.02
	Average**	3.37	32.85	28.27

Al has a detrital and/or volcanic origin. In a marine environment Al a) may be adsorbed on biogenic silica that will be released upon dissolution (Hydes 1977) and MacKenzie et al. (1978), b) may enter the oceans from rivers and be deposited on the seafloor in the form of amorphous Al-hydroxides adsorbed on other particles, c) may be released during alteration of fine-grained volcanic dust particles in the sediment (Hein et al. 1979).

The contribution of intermediate-mafic volcanism is evident in the Karadere Formation in the Mastarhill and Yukarıbağ sections, which have similar geochemical characteristics. Nevertheless, the concentrations of Fe, K, Mn, V, Cu, Pb and As are higher in the Yukarıbağ section.

Manganiferous sample Y2 is significantly enriched in all elements except for Al, Si and Mg and is poor in Ba. Concentrations of P, Mn, Co, Ni, Cu, Ni, Pb and Fe were higher in the Y2 sample than those of other samples. These elements are first adsorbed or co-precipitated onto Mn and Fe oxide films or layers near the sediment surface (Calvert & Price 1970; Duchart et al. 1973). On Fig. 4, all the samples plot in the argillite field whereas the manganiferous Y2 sample plots in the hydrothermal sediment field (Böström 1973).

The concentration of Ba is very high in the Sebken section (Table 3). Low Ba concentrations in the Mastarhill and Yukarıbağ sections might have resulted from contribution by volcanic material. Ba concentrations in PAAS (Post Archean Average Shale) and NASC (North American Shale Composite) standards are about 600 ppm and they are less than

200 ppm in some volcanic sediments (Peate et al. 1997). In the Mastarhill and Yukarıbağ sections, which were affected by volcanism, the Ba content (average 114 ppm and 155.62 ppm) are lower than standard values.

In shales rich in volcanic material, the Y/Ho ratio is 25–37 (McLennan 1989). The average ratio for samples is 28.2 (Table 3). In Figure 5, the samples are plotted in the Fe-rich field, except for five samples. The Zr/Hf ratio of marine sediments is between 14 and 35 (Plank & Langmuir 1998). Excluding the manganiferous sample Y2, the average Zr/Hf ratio is 32.85 in all samples (Table 3).

In the TiO_2 vs. Zr diagram (Fig. 6), the samples excluding the Y2 manganiferous sample plot in the intermediate and mafic fields. The Th/Sc and Zr/Sc ratios are useful indices of chemical differentiation (Leo et al. 2002). Due to the dominance of neutral-basic volcanism in the study area, Th/Sc and Zr/Sc ratios are not consistent with PAAS composition, which is representative for sediments (Fig. 7). Cr/V vs. Y/Ni ratios are used to identify mafic-ultramafic sources. The studied samples plot between PAAS and ultramafic sources (Fig. 8).

Correlation analysis was performed to reveal any communality of minerals and chemical elements. Some correlation plots for major and trace elements are shown in Figure 9. SiO_2 is positively correlated with Al_2O_3, Na_2O, TiO_2

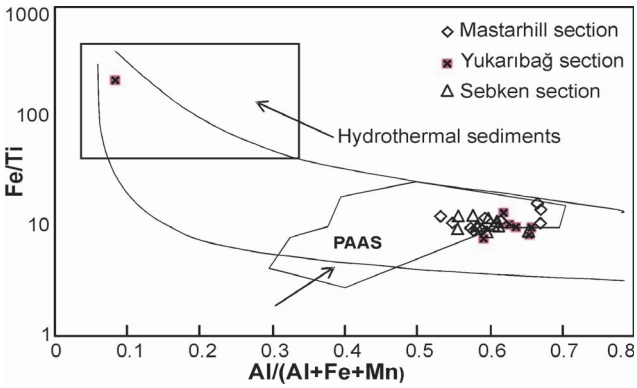

Fig. 4. Böström (1973) diagram. All the samples plot in the argillite field, while manganiferous sample (Y2) is consistent with a hydrothermal origin (PAAS — Post Archaen Average Shale).

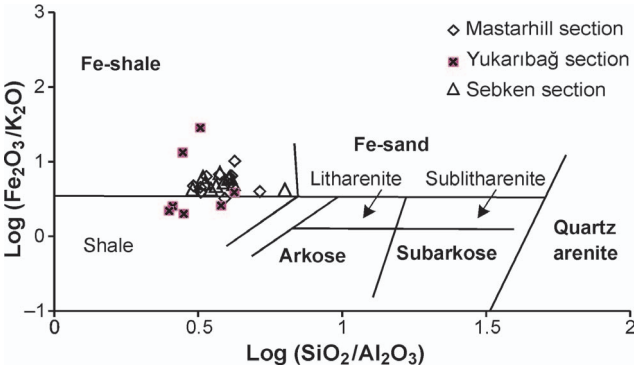

Fig. 5. Log (Fe_2O_3/K_2O) vs. log (SiO_2/Al_2O_3) of samples plotted on geochemical classification diagram after Pettijohn et al. (1972).

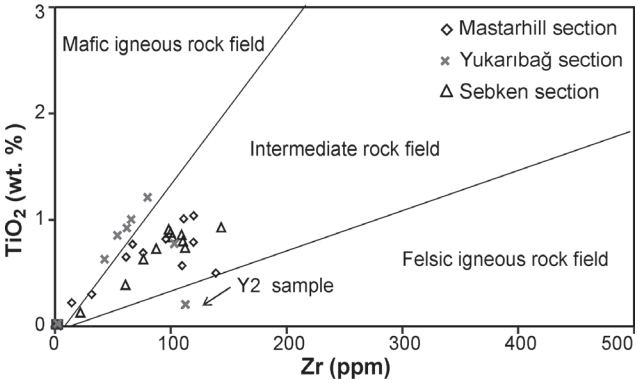

Fig. 6. TiO_2 and Zr content of samples of the Hazar Group–Maden Complex (after Hayashi et al. 2000).

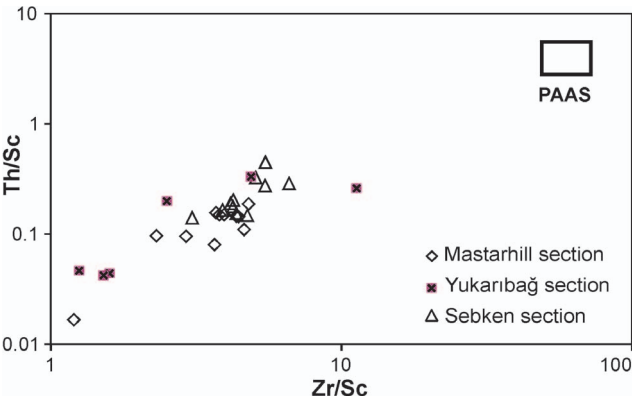

Fig. 7. Th/Sc vs. Zr/Sc diagram of samples.

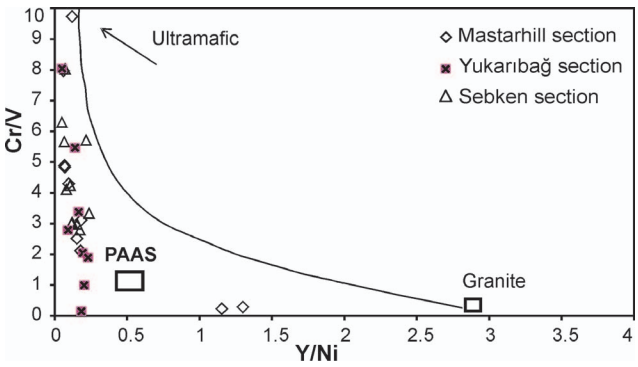

Fig. 8. Cr/V vs. Y/Ni diagram of samples.

(r = 0.42–0.90) and negatively correlated with CaO (r = –0.89). This suggests that CaO is derived primarily from carbonates, and other elements are associated with silicates. Rb is positively correlated with K_2O (r = 0.80) indicating that a similar geochemical behaviour is associated with illite, since both elements are preferentially retained in illite during weathering (Das & Haake 2003). Positive correlations between Ti- and Sc, Co (r = 0.79, 0.56), and between Nb- and Ta, Th, (r = 0.96–0.64) suggest that Ti- and Nb-bearing minerals may at least partially control the distribution of certain trace ele-

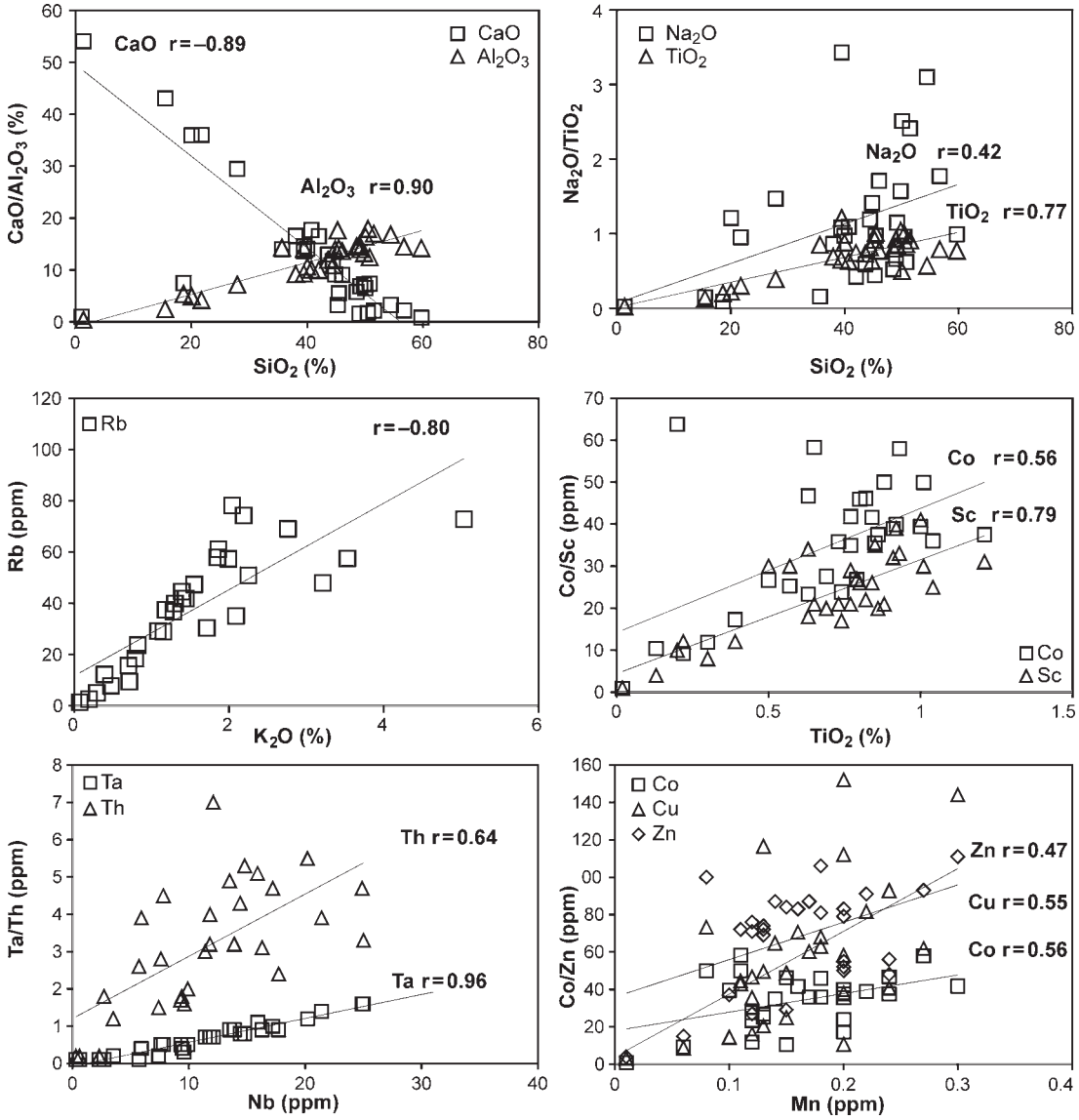

Fig. 9. Correlation between major and trace elements of the analysed sedimentary rocks (the significance level is $\alpha = 0.05$ for correlation coefficient r).

ments (Lopez et al. 2005). Cu, Zn and Co elements show a positive correlation with Mn (r>0.47) and are associated with Mn in the nodules. Mn nodules are known to have a high adsorption capacity for many trace elements in seawater (Calvert & Price 1970; Duchart et al. 1973).

Application of the factor analysis technique yields a considerable reduction in the number of variables and the detection of structure in the relationships between metals. The results, presented as factor loadings of the rotated matrix, are shown in Table 4. Factor 1 reflects Mn, Fe and Ni, Co, Ga, U, V, Y, Mo, Cu, Pb, Zn, As associations and associations of Fe and Mn oxide transition metals as well. Fe and Mn oxides are known to be carriers of transitional metals (Tessier et al. 1992). Factor analysis also differentiates silicates from oxides. In factor 2, the absence of a clear association of SiO_2, Al_2O_3, K_2O, TiO_2, Cs, Hf, Nb, Rb, Ta, Th, Zr and MnO and Fe_2O_3 indicates differentiation between silicates and Fe-Mn oxides.

Rare earth elements

REE concentrations of the three sections are shown in Table 5. REEs are especially useful for monitoring source area composition (Taylor & Mc Lennan 1985; Das et al. 2006). These elements have short residence time in the water column, and thus are transferred almost completely into the sedimentary record and are useful for differentiating felsic from mafic source components in shales (Fedo et al. 1996; Bauluz et al. 2000).

The negative Eu anomaly is more common in continental detrital rocks since their Eu anomaly is generally larger than that of mid-ocean ridge basalts (MORB) (Murray et al. 1992; Das et al. 2006). A negative Eu anomaly may also indicate magmatic fractionation and the presence of evolved rocks (McLennan 1989). Basic rocks contain low $LREE_N/HREE_N$ ratios and no Eu anomalies, whereas more silicic rocks usu-

ally contain higher $LREE_N/HREE_N$ ratios and Eu anomalies (Nyakairu & Koeberl 2001). REE concentrations of whole-rock samples are normalized to chondrite values and it was determined that low LREE concentrations are enriched in comparison to HREEs, and the absence of Eu anomalies shows that our samples are generally mafic in composition, except for a slight Eu peak in the Sebken section (Fig. 10). In the chondrite normalized diagram, the Eu anomaly in Sebken is more significant than in the other two sections, which is indicative of a terrestrial contribution at that site. The presence of a significant Eu depletion reflects high-temperature hydrothermal alteration of the precursor minerals (Lackschewitz et al. 2000). The negative Eu anomaly in sample Y2 and the absence of a significant anomaly in others suggests that these sediments were not affected by hydrothermal alteration. Altunbey & Sağıroğlu (1995) studied Mn mineralization in the vicinity area. They suggest that there is no relation between hydrothermal mineralization and wall-rock composition.

Table 4: Results of factor analysis (n = 30). Bold numbers indicate positive factor loadings (> 0.60). Negative factors shown in box.

	Factor 1	Factor 2	Factor 3	Factor 4	Factor 5
SiO_2	–0.09	**0.95**	0.03	0.25	0.10
Al_2O_3	–0.08	**0.89**	0.18	–0.34	0.10
Fe_2O_3	**0.97**	0.12	0.08	–0.11	0.03
MgO	–0.12	**0.50**	0.71	0.22	–0.09
CaO	–0.30	–0.91	–0.15	0.14	–0.04
Na_2O	–0.20	0.28	0.19	0.33	**0.77**
K_2O	–0.15	**0.64**	–0.04	–0.45	–0.25
TiO_2	–0.12	**0.83**	0.27	0.27	–0.04
P_2O_5	**0.98**	–0.10	0.01	–0.07	–0.05
MnO	**0.96**	–0.22	–0.01	–0.09	0.02
Cr_2O_3	–0.04	0.22	**0.62**	0.47	–0.23
Ni	**0.74**	0.11	0.31	–0.02	–0.24
Sc	–0.10	**0.78**	0.40	–0.43	0.01
Ba	–0.14	–0.11	–0.36	–0.09	–0.44
Co	**0.55**	**0.61**	0.43	0.15	–0.23
Cs	–0.05	**0.73**	–0.34	0.05	–0.40
Ga	**0.77**	**0.57**	0.01	–0.19	–0.01
Hf	0.10	**0.85**	–0.32	0.25	0.27
Nb	0.02	**0.77**	–0.25	0.48	0.27
Rb	–0.12	**0.82**	–0.27	–0.40	–0.34
Sr	–0.06	–0.73	0.10	0.39	0.27
Ta	–0.64	**0.72**	–0.35	0.34	0.31
Th	0.14	**0.67**	–0.47	–0.09	–0.17
U	**0.84**	0.05	–0.26	–0.11	–0.05
V	**0.98**	–0.04	0.07	–0.08	0.10
Zr	0.36	**0.80**	–0.25	0.21	0.24
Y	**0.98**	–0.04	–0.04	0.02	0.08
Mo	**0.94**	–0.23	–0.01	–0.19	0.02
Cu	**0.96**	–0.10	0.04	–0.14	–0.01
Pb	**0.97**	–0.19	–0.05	–0.16	–0.01
Zn	**0.99**	0.03	–0.05	0.01	0.07
As	**0.96**	–0.20	–0.02	–0.06	0.03
Eigenvalues	12.11	10.32	2.51	2.22	1.79
Accumulated variance (%)	37.9	70.1	78.0	84.9	90.6

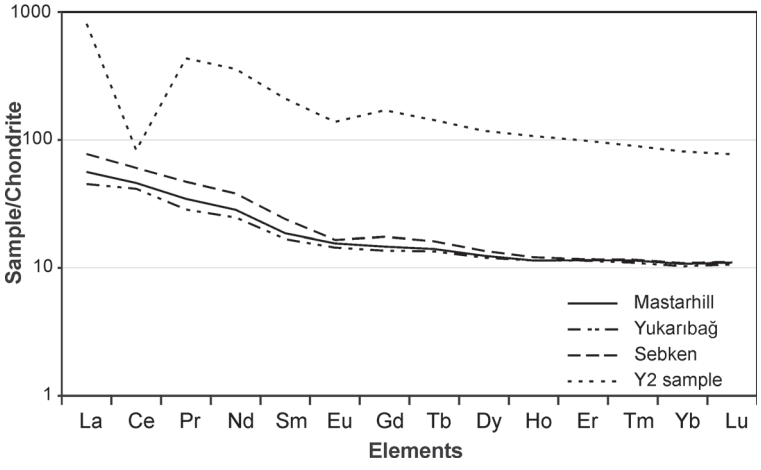

Fig. 10. Chondrite-normalized REE patterns for the Sebken, Mastarhill and Yukarıbağ sections and Y2 manganiferous sample.

Fe-Mn oxides with negative Ce anomalies are also known from hydrothermal precipitates (Halbach et al. 1989; Hein et al. 1990). A hydrothermal REE signature, characterized by a prominent negative Ce anomaly and a typically high La value is shown in the Y2 manganese sample (Fig. 10). On the other hand, a negative Ce anomaly is common in marine environments due to the oxidation of Ce^{3+} to Ce^{4+} by Mn (McLennan 1989). The deficiency of Ce relative to neighbouring rare earth elements is an important feature of modern seawater. This can be explained by the oxidation of trivalent Ce to less soluble tetravalent Ce and by the successive removal by suspended particles through the scavenging process (Sholkovitz et al. 1994). However, Ce is remobilized and released into the water column in the suboxic environment resulting in a less negative to positive anomaly in seawater (De Baar 1991). The absence of a Ce anomaly in all samples except for sample Y2 might indicate a suboxic character of the environment.

The REE show a moderate correlation (r) with MnO (between 0.46–0.60) and P_2O_5 (between 0.37–0.72) (Table 6, Fig. 11). Sample Y2 is composed of Mn-rich nodules and this sample has very high REE values. Mn nodules in oceanic sediments are thought to be effective in concentrating REE in the marine environment (Brokins 1988).

Discussion

Sedimentological findings from the southern and northern parts of Mastar Mountain indicate that the southern branch of the Neotethys Ocean (NE-SW trending Hazar Basin) started to open in the Late Maastrichtian in the continental crust with the formation of the Guleman Ophiolites.

In the first stage of basin formation, flysch deposits of the Simaki Formation were deposited (Sebken section). In the Late Maastrichtian–Middle Eocene, the Gehroz Formation (lower level of Mastarhill section) was deposited. It is the equivalent of the Simaki Formation, and corre-

Table 5: Rare Earth Element contents in samples from the Sebken, Mastarhill and Yukarıbağ sections.

	Concentration (ppm)													
	Sample No.	**La**	**Ce**	**Pr**	**Nd**	**Sm**	**Eu**	**Gd**	**Tb**	**Dy**	**Ho**	**Er**	**Tm**	**Yb**	**Lu**
Sebken	S-1	17.2	35	4.48	18.6	4.39	1.23	4.44	0.75	4.48	0.94	2.6	0.41	2.52	0.39
	S-4	22.3	46.4	5.04	20.5	4.2	1.04	3.91	0.64	3.83	0.76	2.15	0.34	2.12	0.32
	S-9	19.1	37.3	4.68	17.8	3.5	0.71	3.39	0.58	3.27	0.66	1.86	0.3	1.85	0.28
	S-12	14.8	30.2	3.49	13.4	2.84	0.75	2.77	0.48	2.79	0.56	1.58	0.24	1.59	0.24
	S-14	22.1	48.7	5.18	20.2	4.04	1.15	3.9	0.64	3.65	0.69	1.97	0.29	1.84	0.29
	S-16	25.6	56.4	6.56	26.4	5.4	1.53	5.42	0.9	5.1	0.97	2.82	0.42	2.42	0.37
	S-20	17.3	36.8	4.21	16.9	3.43	0.98	3.35	0.57	3.11	0.62	1.74	0.26	1.72	0.25
	S-28	16.6	27.9	4.17	17.1	3.34	0.8	3.12	0.51	2.9	0.55	1.58	0.23	1.5	0.23
	S-38	11.6	10.9	2.56	10.2	2.06	0.47	2.12	0.32	1.88	0.38	1.03	0.16	0.98	0.14
	S-41	16.1	33.5	4.03	16.1	3.4	0.87	3.44	0.61	3.44	0.68	1.94	0.29	1.88	0.28
	S-44	19	42	4.69	18.1	3.72	1.01	3.66	0.64	3.6	0.74	2.07	0.32	2	0.33
	Average	18.33	36.82	4.46	17.75	3.66	0.95	3.59	0.60	3.45	0.68	1.94	0.29	1.85	0.28
Mastarhill	M-1	1.6	3	0.49	2.5	0.68	0.25	1	0.17	1.01	0.24	0.73	0.09	0.63	0.10
	M-4	10.5	21.4	2.53	10.1	2.11	0.68	2.31	0.41	2.56	0.48	1.42	0.21	1.33	0.20
	M-6	15.1	30.2	3.65	14.9	3.01	0.98	3.16	0.52	3	0.62	1.78	0.26	1.7	0.25
	M-7	17	33.6	3.94	15.8	3.34	0.93	3.47	0.6	3.42	0.71	1.94	0.3	1.82	0.27
	M-9	5.3	10.9	1.36	6.5	1.34	0.38	1.35	0.23	1.51	0.28	0.83	0.13	0.8	0.12
	M-13	18.2	39.4	4.61	18.4	3.98	0.93	4.1	0.7	4.05	0.81	2.41	0.38	2.25	0.36
	M-17	11.5	22.8	2.82	12.1	2.66	0.84	2.92	0.52	3.12	0.64	1.93	0.29	1.92	0.28
	M-19	20.5	45.7	4.98	19	3.82	1.05	3.77	0.63	3.65	0.75	2.19	0.33	2.05	0.3
	M-21	16.1	36.3	4.16	16.5	3.68	0.88	3.94	0.72	4.61	0.94	2.81	0.44	2.76	0.44
	M-24	12.4	26.8	3.16	13.1	3.01	0.85	3.37	0.63	4.1	0.84	2.49	0.4	2.54	0.4
	M-25	17.9	39.4	4.4	16.9	3.66	0.97	3.77	0.65	3.77	0.8	2.38	0.38	2.32	0.36
	Average	13.28	28.13	3.28	13.25	2.84	0.79	3.01	0.52	3.16	0.64	1.90	0.29	1.82	0.28
Yukarıbağ	Y-1	3.7	10.8	1.76	9.00	2.85	1.04	3.55	0.67	4.01	0.86	2.47	0.35	2.18	0.34
	Y-2	191.8	50.7	41.26	167.5	32.19	8.02	35.03	5.33	29.85	6.06	16.38	2.29	13.79	1.96
	Y-3	18.2	49	4.61	18.3	3.84	0.9	3.62	0.59	3.56	0.72	2.12	0.31	2.11	0.31
	Y-4	14	26.8	3.03	12.9	2.28	0.74	2.22	0.38	2.23	0.49	1.44	0.22	1.21	0.21
	Y-11	9	22.9	2.19	9.5	2.14	0.79	2.46	0.46	2.88	0.61	1.69	0.25	1.64	0.23
	Y-12	9.4	21.7	2.19	9.4	2.11	0.75	2.28	0.45	2.86	0.62	1.82	0.28	1.76	0.27
	Y-14	9.8	20.8	2.44	10.0	2.19	0.79	2.67	0.47	2.79	0.58	1.79	0.27	1.61	0.26
	Y-16	1.5	1.2	0.28	1.10	0.24	0.06	0.29	0.04	0.22	0.07	0.19	0.02	0.13	0.02
	Average	32.17	25.48	7.22	29.71	5.98	1.63	6.51	1.04	6.05	1.25	3.48	0.49	3.05	0.45

Table 6: Correlation coefficients between REE and MnO and P_2O (the significance level is $\alpha = 0.05$ for correlation coefficient r).

	La	**Ce**	**Pr**	**Nd**	**Sm**	**Eu**	**Gd**	**Tb**	**Dy**	**Ho**	**Er**	**Tm**	**Yb**	**Lu**
P_2O_5	0.69	0.68	0.69	0.72	0.68	0.70	0.63	0.58	0.50	0.46	0.43	0.41	0.37	0.37
MnO	0.47	0.50	0.51	0.55	0.57	0.60	0.56	0.54	0.53	0.52	0.51	0.48	0.46	0.46

sponds to deeper parts (slope) of the Hazar Basin further to the east. In the Middle Eocene, development of the Hazar Basin was accelerated and basaltic-andesitic volcanism, known as the Karadere Formation (upper level of Mastarhill section), was formed towards the east. Following this volcanism an embryonic stage of ocean opening (Yukarıbağ section) resulted in Mn mineralization.

Origin of smectites

Several types of gneiss are related to the origin of smectites in marine sediments, such as reworked soils, transportation of detrital smectite from soils and alteration of volcanic rocks.

Reworked smectitic soils and vertisols may be a potential source for detrital input from continent to marine environment, but Thiry (2000) objects that smectitic soils are relatively scarce. Well-developed smectitic soils are mostly restricted to dry tropical climates along with poorly drained landscapes. Accordingly, these soils are shallow and contribute only small amounts to inherited materials. Vertisols contain kaolinite (Chamley 1989). Bolle et al. (2000) found that warm and humid climate conditions are ascendant in the Tethyan margin during the Paleocene, as indicated by the abundance of kaolinite in vertisols. According to Thiry (2000), the marine sediments do not contain detrital kaolinite inherited from continental areas and therefore cannot be used to explain smectite deposits in the ocean. Therefore, input of smectite from marine volcanic rocks is expected to be the main source of smectite.

Volcanogenic smectite forms either from the alteration of marine volcanic material or from only slightly weathered volcaniclastic sediments (Worden & Morad 2003). Smectite-rich marine sediments were deposited along the southeastern Neotethys margin during the oceanic convergence stage in the Senonian–Eocene period (Shoval 2004). The sediments in the Hazar-Maden Basin are the equivalent of those deposited in Neotethys. The origin of smectite is more controversial as these minerals characterize either volcanic environments, restricted evaporative environments or may be derived from

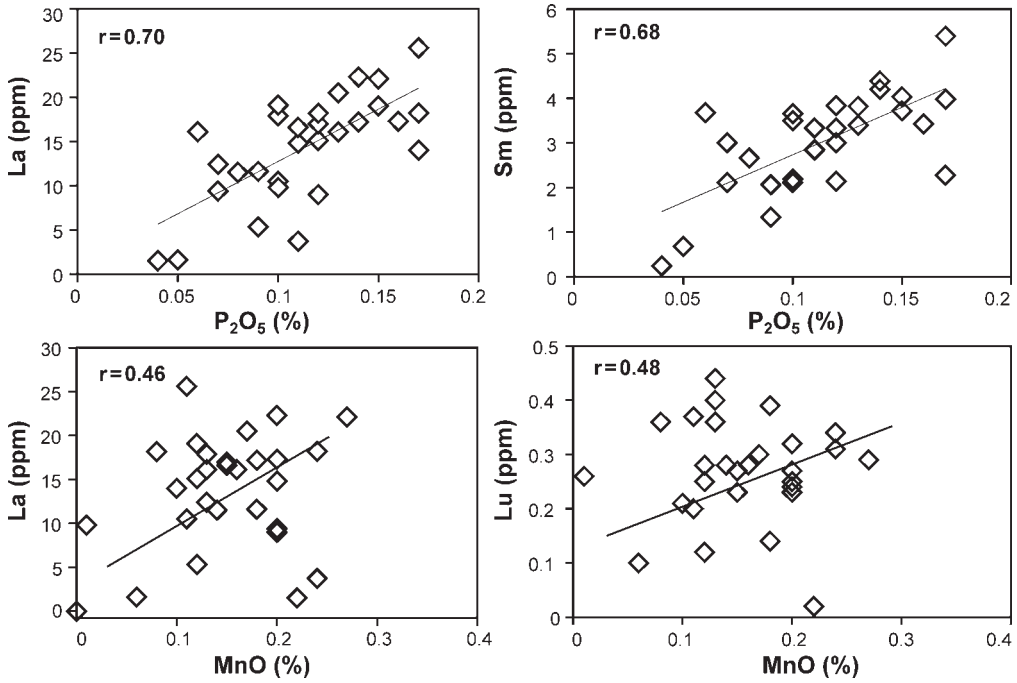

Fig. 11. Correlation between REE and MnO and P_2O (the significance level is $\alpha = 0.05$ for correlation coefficient r).

the erosion of soils (Hein et al. 1979; Chamley 1989). According to Shoval (2004), a smectite–opal-CT association reflects a marine origin. In scanning electron microscope studies, it was observed that smectite has a well developed platy structure and honeycomb texture morphology (Fig. 5a). In general, smectite develops in fissures, fractures and dissolution voids of volcanic glass (Fig. 5b) as well as on and along the edges of feldspar. This may indicate that volcanic glass exerted a major control in smectite formation.

Distribution of element ratios in the basin

Y, Sc, Cr, Th, Sc and Co are relatively immobile elements in sedimentary processes. Therefore they are useful for provenance characterization (Cullers & Stone 1991; Bauluz et al. 2000; Lopez et al. 2005). These elements are believed to be transported exclusively in terrigenous components of the sediment and, therefore, they reflect the chemistry of their source rocks (Rollison 1993). Th/U, Sc/Th, La/Sc, Co/Th, and ratios of immobile elements are also used to determine source rocks (Taylor & McLennan 1985).

Th concentrations indicate a higher proportion of felsic material in their source area (Bauluz et al. 2000). The Th/U ratio is high in the Sebken section (average 4.35) where terrigenous contribution is also high, but it is low in the Mastarhill and Yukarıbağ section (average 2.93 and 2.61 respectively), which is dominated by a contribution from basic rocks (Table 3). The Sc/Th ratio in the Sebken section is consistent with an andesitic composition (average 4.96), in the Mastarhill section it indicates andesitic-basaltic composition (average 12.84), and in the Yukarıbağ section it is typical of basic and ophiolitic rocks (average 32.14) (Table 7). The La/Sc ratio in Sebken is consistent with andesitic-basaltic composition. This ratio is highest in the Sebken section (average 1.07) where the terrigenous contribution is higher (Table 7). The average Co/Th ratio in the Sebken section is consistent with a basic composition (average 8.42) while in the Mastarhill and Yukarıbağ sections it ranges between basic and ophiolitic rock composition (average 14.99 and 40.09, respectively) (Table 7).

The ∑REE value is higher in the Yukarıbağ section, which is dominated by both basic and hydrothermal contributions (Table 8). The Yb_N/Sm_N ratio is 0.50 in the Sebken section and 0.64 and 0.66 in the Yukarıbağ and Mastarhill sections respectively. These ratios are conformable with the differentiation of terrestrial detritals and arc volcanic contributions (Plank & Langmuir 1998). While the Sm_N/Nd_N ratio is lower, the La_N/Yb_N, La_N/Sm_N, $LREE_N/HREE_N$ ratios are higher in the Sebken section in comparison to the Yukarıbağ and Mastarhill sections (Table 8). This indicates that the contribution

Table 7: Elemental ratios in the Hazar Group–Maden Complex. Bold numbers indicate higher ratio.

	Sebken (n=11)	Mastarhill (n=11)	Yukarıbağ (n=8)	Andesites[a]	Basic rocks[b]	Ophiolites[c]
Sc/Th	4.96 (2.22–7.11)	12.84 (5.31–60)	**32.14 (3–55)**	4.65	20–25	56
Co/Th	8.42 (4.43–16.12)	14.99 (6.87–46)	**40.09 (4.5–187)**	4.65	7.1–8.3	70
La/Sc	**1.07 (0.52–2.9)**	0.56 (0.13–0.82)	0.51 (0.11–1.5)	0.9	0.4–1.1	0.25

[a] — Condie (1993), [b] — Cullers at al. (1988), [c] — Spadea et al. (1982).

from continental source rocks increases in the Sebken units (Plank & Ludden 1992) (Fig. 12).

Conclusions

Andesitic-basaltic rocks have been altered under marine conditions in the Hazar-Maden Basin. The nature of the clay minerals is controlled by these volcanic rocks. Volcanogenic iron-rich smectites, S-C and chlorite are dominant in the basin along with illite, palygorskite, I-S and I-C.

Samples of the Upper Maastrichtian–Middle Eocene Hazar Group and the Middle Eocene Maden Complex from the Hazar-Maden Basin were studied to investigate the main effects of depositional environmental parameters in three sections belonging to deeper marine (slope) and proximal arc volcanic (Mastarhill and Yukarıbağ sections) and shallow platform marine (Sebken section) settings. In the chondrite normalized diagram, the Eu anomaly in Sebken is more significant than in the other two sections, but the Th/U, La/Sc, La_N/Yb_N, La_N/Sm_N, $LREE_N/HREE_N$ ratios are slightly higher in the Sebken section in comparison to the Yukarıbağ and Mastarhill sections, which is indicative of a terrestrial contribution at Sebken showing little detritic smectite contribution. On the other hand, smectite soils are shallow of origin and contribute only small amounts to inherited materials. During the development of the Hazar-Maden Basin, abundance of kaolinite in the vertisols and the absence of kaolinite in sediments show the low detritic contribution to the basin. The Sc/Th, Co/Th ratios are consistent with the basic type volcanism and increase from the Sebken to the Mastarhill and Yukarıbağ sections. The smectite-opal-CT association is especially abundant in the samples taken from the Sebken and Yukarıbağ sections. The Mg/(Fe+Mg) ratio is 0.4–0.75 in octahedral cations, and it can be attributed to trioctahedral smectite with Fe-saponite composition. The chemical composition of smectite shows high Mg, Fe, Ni and Cr concentrations, which are present in octahedral sites and these results might indicate that the smectite is formed from basaltic rocks as the Fe-rich gels

Table 8: REE elemental ratios in the Hazar Group–Maden Complex. N — Chondrite normalized values, n — Sample number. Bold numbers indicate higher ratio.

	Sebken	Mastarhill	Yukarıbağ
	Range (n=11)	**Range (n=11)**	**Range (n=8)**
ΣREE	6.77 (0.14–56.4)	5.23 (0.09–45.7)	**8.90 (0.02–191.8)**
Yb_N/Sm_N	0.50(0.44–0.55)	0.66 (0.53–0.92)	0.64(0.53–0.83)
Sm_N/Nd_N	2.62 (1.90–3.90)	4.22 (2.38–14.20)	6.83 (0.79–31.05)
La_N/Yb_N	**12.25 (10.91–13.78)**	11.45 (10.10–12.80)	11.75 (10.59–15.23)
La_N/Sm_N	**23.50 (6.22–31.07)**	20.67 (0.31–31.38)	17.71 (0.66–35.24)
$LREE_N$ / $HREE_N$	**66.22 (44.10–82.86)**	46.66 (16.00–68.32)	52.59 (10.88–97.86)

Chondrite values from Taylor & McLennan (1985); Shale values from Piper (1974).

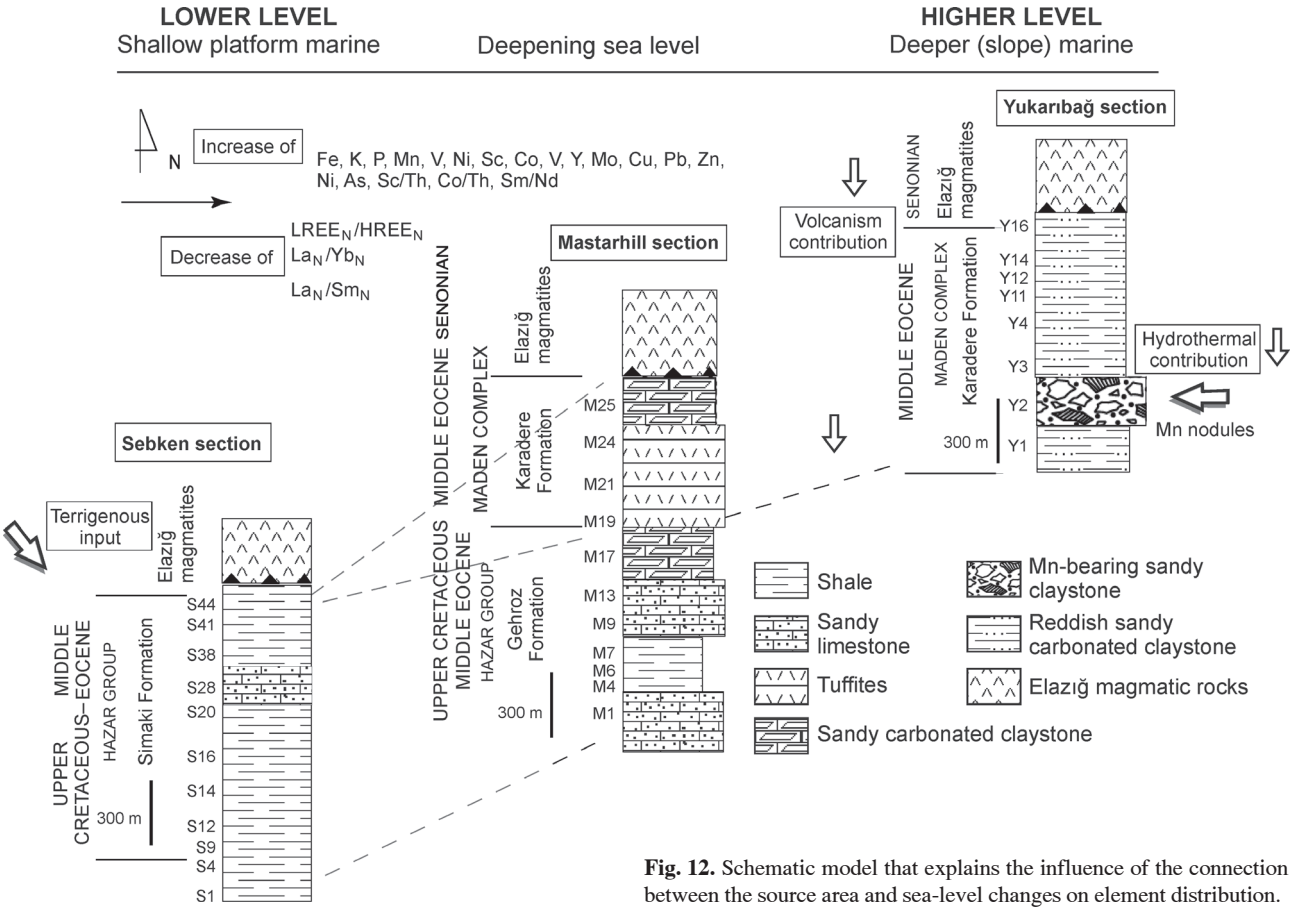

Fig. 12. Schematic model that explains the influence of the connection between the source area and sea-level changes on element distribution.

react with solid particles and dissolved species. In addition, in scanning electron microscope studies, the presence of well developed honeycomb texture morphology reflects authigenic formation which may indicate that volcanic glass exerted a major control in smectite formation.

These data are consistent with previous stratigraphic findings and petrographic studies in the basin. On a regional scale, the equivalents of these units are widespread and a mineralogical-geochemical study of these marine sediments can be used to add new insights into the Cenozoic stratigraphic evolution.

Acknowledgments: We are grateful to Prof. George E. Christidis, Technical University of Crete (Greece), Prof. Hüseyin Yalçın, Cumhuriyet University (Turkey), for editorial comments. The financial support of the Fırat University (Turkey) Scientific Research Projects Unit under FUBAP-1805 project number is gratefully acknowledged. We would like to thank ACME (Canada) and General Directorate of Mineral Research & Exploration (Ankara, Turkey) for chemical and mineralogical analysis. We are grateful to Prof. Paul A. Schroeder, University of Georgia, (USA), Prof. Asuman Günal Turkmenoğlu, Middle East Technical University (Turkey), and RNDr. Jaroslav Lexa, Geological Institute, Slovak Academy of Sciences, whose helpful reviews have greatly improved the manuscript.

References

Aktaş G. & Robertson A.H.F. 1990: Tectonic evolution of the Tethys suture zone in SE, Turkey: Evidence from the petrology and geochemistry of Late Cretaceous and Middle Eocene extrusives. In: Symp. on ophiolite genesis and evolution of oceanic lithosphere. *Geol. Soc. London, Spec. Publ.,* 311–328.

Altunbey M. & Sağıroğlu A. 1995: Properties and origin of Koçkale-Elazığ Manganese deposits. *MTA J.* 117, 139–148.

Bauluz B., Mayayo M.J., Fernandez-Nieto C. & Lopez J.M.G. 2000: Geochemistry of Precambrian and Paleozoic siliciclastic rocks from the Iberian Range (NE Spain): implications for source-area weathering, sorting, provenance, and tectonic setting. *Clays and Clay Miner.* 48, 374–384.

Bhatia M.R. & Crook A.W. 1986: Trace element characteristics of graywackes and tectonic setting discrimination of sedimentary basins. *Contr. Mineral. Petrology* 92, 181–193.

Bolle M.P., Pardo A., Adatte T., Von Salis K. & Burns S. 2000: Climatic evolution on the southeastern margin of the Tethys (Negev, Israel) from the Paleocene to the early Eocene: Focus on the late Paleocene thermal maximum. *J. Geol. Soc. London* 157, 929–941.

Böström K. 1973: The origin and fate of ferromanganoan active ridge sediments. *Stockholm Contr. Geol.* 27, 149–243.

Brindley G.W. 1980: Order-disorder in clay mineral structures. In: Brindley G.W. & Brown G. (Eds.): Crystal structures of clay minerals and their X-ray identification. *Mineral. Soc.,* London, 125–195.

Brookins D.G. 1988: Eh-PH diagrams for geochemistry. *Springer-Verlag,* Berlin, 1–176.

Calvert S.E. & Price N.B. 1970: Composition of manganese nodules and manganese. Carbonates from Loch Fyne, Scotland. *Contr. Mineral. Petrology* 29, 215–233.

Condie K.C. 1993: Chemical composition and evolution of the upper continental crust: contrasting results from surface samples and shales. *Chem. Geol.* 104, 1–37.

Cullers R.L. & Stone J. 1991: Chemical and mineralogical comparison of the Pennsylvanian fountain formation, Colorado, USA (an uplifted continental block) to sedimentary-rocks from other tectonic environments. *Lithos* 27, 115–131.

Cullers R.L., Basu A. & Suttner L.J. 1988: Geochemical signature of provenance in sand-size material in soils and stream sediments near the Tobacco Root batholith, Montana, USA. *Chem. Geol.* 70, 335–348.

Chamley H. 1989: Clay sedimentology. *Springer-Verlag,* Berlin, 1–623.

Chen S.Y., Takematsu N., Ambe S., Ament A. & Ambe F.A. 1994: Mösseauer spectroscopy study on iron in marine sediments. *Hyperfine Interactions* 91, 759–763.

Christidis G.E. & Huff W.D. 2009: Geological aspects and genesis of bentonites. *Elements* 5, 93–98.

Christidis G., Scott P.W. & Markopoulos T. 1995: Origin of the bentonite deposits of Eastern Milos, Aegean, Greece: Geological, mineralogical and geochemical evidence. *Clays and Minerals* 43, 63–77.

Çelik H. 2003: Stratigraphic and tectonic features of vicinity of Mastar Mountain (SE of Elazığ). *PhD. Thesis, Fırat University,* 1–95 (in Turkish).

Das B.K. & Haake B. 2003: Geochemistry of Rewalsar Lake sediment, Lesser Himalaya, India: implications for source-area weathering, provenance and tectonic setting. *Geosci.* 7, 299–312.

Das B.K., Mikhlafi A.S. & Kaur P. 2006: Geochemistry of Mansar Lake sediments, Jammu, India: Implication for source-area weathering, provenance, and tectonic setting. *Earth Sci.* 26, 649–668.

De Baar H.J.W., Schijf J. & Byme R.H. 1991: Solution chemistry of the rare earth elements in seawater. *Eur. J. Solid State lnorg. Chem.* 28, 357–373.

Duchart D., Cakmt S.E. & Price N.B. 1973: Distribution of trace metals in the pore waters of shallow water marine sediments. *Limnology and Oceanography* 18, 4, 605–610.

Erdem E. 1987: Petrological investigation of magmatic rocks around Elazığ Kartaldere-Gölardı (NE of Hazar Lake). *Master Thesis, Fırat Univ.,* 1–72 (in Turkish).

Erdoğan B. 1977: Geology geochemistry and genesis of the sulphide deposits of the Ergani-Maden region SE Turkey. *PhD. Thesis, New Brunswick Univ. Canada,* 1–156.

Fedo C.M., Eriksson K. & Krogstad E.J. 1996: Geochemistry of shale from the Archean (~3.0 Ga) Buhwa Greenstone belt, Zimbabwe: Implications for provenance and source area weathering. *Geochim. Cosmochim. Acta* 60, 10, 1751–1763.

Gündoğdu M.N. 1982: Geological, mineralogical and geochemical investigation of Neogene Bigadiç Basin. *PhD. Thesis, Hacettepe Univ.*, 1–386 (in Turkish).

Halbach P., Kriete C., Prause B. & Puteanus D. 1989: Mechanisms to explain the platinu concentration in ferromanganese seamount crusts. *Chem. Geol.* 76, 95–106.

Hayashi M., Komiya T., Nakamura Y. & Maruyama S. 2000: Archean regional metamorphism of the Isua supracrustal belt, southern West Greenland: implications for a driving force of Archean plate tectonics. *Int. Geol. Rev.* 42, 1055–1115.

Hein J.R., Hsueh-Wen Yeh Z. & Alexander E. 1979: Origin of iron-rich montmorillonite from the Manganese nodule belt of the North equatorial pacific. *Clays and Clay Miner.* 27, 185–194.

Hein J.R., Kirschenbaum H., Schwab W.C., Usui A., Taggart J.E., Stewart K.C., Davis A.S., Terashima S., Quinterno P.J., Olson R.L., Pickthorn L.G., Schulz M.S. & Morgan C.L. 1990: Mineralogy and geochemistry of Co-rich ferromanganese crusts and substrate rocks from Karin Ridge and Johnston Island. *Farnella Cruise F7-86-HW. U.S. Geol. Surv. Open File Report,* 90–298.

Hempton M. 1984: Results of detailed mapping near Lake Hazar

Eastern Taurus mountains. *Geol. Taurus Belt Proceedings of International Tauride Symposium,* 223–228.

Huff W.D. 2006: Volcanism and its contribution to mudrock genesis. *Turkish J. Earth Sci.* 15, 111–122.

Huff W.D. & Turkmenoglu A.G. 1981: Chemical characteristics and origin of Ordovician K-bentonites along the Cincinnati Arch. *Clays and Clay Miner.* 29, 113–123.

Hydes D.J. 1977: Dissolved aluminum concentration in seawater. *Nature* 268, 136–137.

Ileri S., Salancı B., Bitem M. & Doğan R. 1976: Ergani (Maden) copper deposits and plate tectonic. *Bull. TJK* 19, 133–142.

Kaiser H.F. 1960: The application of electronic computers to factor analysis. *Educational and Psychological Measurement* 20, 141–151.

Köster H.M., Ehrlicher U., Gilg H.A., Jordan R., Murad E. & Onnich K. 1999: Mineralogical and chemical characteristics of five nontronites and Fe-rich smectites. *Clays and Clay Miner.* 34, 579–599.

Lackschewitz K.S., Singer A., Botz R., Garbe-Schönberg C.D., Stoffers P. & Hortz K. 2000: Formation and transformation of clay minerals in the hydrothermal deposits of Middle Valley, Juan de Fuca Ridge, ODP Leg 169. *Econ. Geol.* 95, 361–390.

Lanson B., Sakharov B.A., Claret F. & Drits V.A. 2009: Diagenetic smectite-to-illite transition in clay-rich sediments: a reappraisal of X-ray diffraction results using the multi-specimen method. *Amer. J. Sci.* 309, 476–516.

Leo D.P., Dinelli E., Mongelli G. & Schiattarella M. 2002: Geology and geochemistry of Jurassic pelagic sediments, Scisti silicei Formation, southern Apennines, Italy. *Sed. Geol.* 150, 229–246.

Lopez J.M.G., Bauluz B., Yuste A., Mayayom M.J. & Fernandez-Nieto C. 2005: Mineralogical and trace element composition of clay-sized fractions from Albian siliciclastic rocks (Oliete Basin, NE Spain). *Clay Miner.* 40, 565–580.

MacKenzie F.T., Stoffyn M. & Wollast R. 1978: Aluminum in seawater: control by biological activity. *Science* 199, 680–682.

McLennan S.M. 1989: Rare earth element in sedimentary rocks. In: Lipin B.R. & McKay G.A. (Eds.): Influence of provenance and sedimentary processes geochemistry and mineralogy of rare earth elements. *Mineral. Soc. Amer.,* 169–200.

Moore D. & Reynolds C. 1989: X-Ray diffraction and the identification and analysis of clay minerals. *Oxford University Press,* 1–332.

Murray R.W., Bucholtzten Brink M.R., Gerlach D.C., Russ G.P. & Jones D.L. 1992: Interoceanic variations in the rare earth, major, and trace element depositional chemistry of chert: perspectives gained from the DSDP and ODP record. *Geochim. Cosmochim. Acta* 56, 1897–1913.

Özçelik M. 1982: The petrology and geochemistry of volcanic rocks and associated sulphide deposits of the SE Anatolian ophiolite belt, near Malatya, Turkey. *Unpubl. Ph.D. Thesis, Univ. Durham, UK,* 1–453.

Özçelik M. 1985: Geology of the Maden magmatic rocks, southeast Malatya, and a geochemical approach to their tectonic setting. *Bull. TJK* 28, 19–36.

Özkan Y.Z. & Öztunalı Ö. 1984: Petrology of the magmatic rocks of Guleman Ophiolite. *Int. Symp. Geol. Taurus Belt,* Ankara, 285–294.

Peate D.W., Pearce J.A., Hawkesworth C.J., Colley H., Edwards C.M.H. & Hirose K. 1997: Geochemical variations in Vanuatu arc lavas: the role of subducted material and a variable mantle wedge composition. *J. Petrology* 38, 1331–1358.

Pettijohn F.H., Potter P.E. & Siever R. 1972: Sand and sandstone. *Springer-Verlag*, 1–618.

Piper D.Z. 1974: Rare earth elements in the sedimentary cycle, a summary. *Chem. Geol.* 14, 285–304.

Plank T. & Langmuir C.H. 1998: The chemical composition of subducting sediment and its consequences for the crust and mantle. *Chem. Geol.* 145, 325–394.

Plank T. & Ludden J.N. 1992: Geochemistry of sediments in the Argo abyssal plain at site 765: a continental margin reference section for sediment recycling in subduction zones. In: Gradstein F.M. & Ludden J.N. et al. (Eds.): Proceedings Ocean Drilling Project. *Scientific Result,* 167–189.

Rigo de Righi M. & Cortesini A. 1964: Gravity tectonics in foothills structure belt of southeast Turkey. *Amer. Petr. Geol. Bull.* 48, 1911–1937.

Rollinson H. 1993: Using geochemical data: evaluation, presentation, interpretation. *Longman Scientific and Technical*, New York, 1–352.

Sholkovitz E.R., Landing W.M. & Lewis B.L. 1994: Ocean particle chemistry: the fractionation of rare earth elements between suspended particles and seawater. *Geochim. Cosmochim. Acta* 58, 1567–1579.

Shoval S. 2004: Clay sedimentation along the southeastern neo-Tethys margin during the oceanic convergence stage. *Applied Clay Sci.* 24, 287–298.

Spadea P. 1982: Continental crust rocks associated with ophiolites in Lucanian Apennine (Southern Italy). *Ofioliti* 7, 501–522.

Taylor S.R. & McLennan S.H. 1985: The continental crust: its composition and evolution. *Blackwell,* Oxford, 1–312.

Tessier D., Rakai A. & Verduraz F.B. 1992: Spectroscopy study of the interaction of carbon monoxide with cationic and metallic palladium-alumina catalysts. *J. Chem. Soc. Faraday Trans.* 88, 741–749.

Thiry M. 2000: Paleoclimatic interpretation of clay minerals in marine deposits: an outlook from the continental origin. *Earth Sci. Rev.* 49, 201–221.

Weaver C.E. & Pollard L.D. 1973: The chemistry of clay minerals. *Elsevier,* Amsterdam, 55–57.

Wiewor I.A. 1978: Ni-containing mixed-layer silicates from Srklary. Lower Silesia. *Poland. Bur. Rmh. Geol. Inin.* 3, 247–261.

Worden R.H. & Morad S. 2003: Clay minerals in sandstones: Controls on formation distribution and evolution. In: Worden R.H. & Morad S. (Eds.): Clay mineral cements in sandstones. *Spec. Publ. Int. Assoc. Sed.,* 3–41.

Yazgan E. 1984: Geodynamic evolution of the Eastern Taurus region (Malatya-Elazığ area, Turkey). *Geol. Taurus Belt Proceedings of International Tauride Symposium. MTA Publications*, Ankara, 199–208.

Yazgan E. & Chessex R. 1991: Geology and tectonic evolution of the southeastern Taurides in the region of Malatya. *Turkish Assoc. Petrol. Geol.* 3, 1–42.

Yılmaz Y. 1993: New evidence and model on the evolution of the Southeast Anatolian orogen. *Geol. Soc. Amer. Bull.* 105, 251–271.